QUANTUM MONTE CARLO IN NUCLEAR PHYSICS

JOSEPH CARLSON
Theoretical Division
Los Alamos National Laboratory
Los Alamos, NM 87545

1. Introduction

Many intriguing nuclear phenomenon are studied using Quantum Monte Carlo methods, including the spectra and structure of light nuclei, electron scattering, the weak parity-violating interactions at the nuclear scale, and the weak-capture reactions that produce solar neutrinos. These are all processes that can be treated using extensions of standard QMC methods and realistic models of the nuclear interaction and current. A review of the field of few-nucleon physics, including Monte Carlo and other methods, is given in a recent Reviews of Modern Physics article.[1]

For larger systems, shell models of nuclei are often used. The shell model of nuclei employs low-energy effective interactions, and is used to study a host of nuclear properties including pairing in nuclei, stability limits in the regime of neutron-rich nuclei, and r-process nucleosynthesis. These effective low-energy interactions can be adapted to Auxiliary-Field Quantum Monte Carlo techniques. Shell Model Monte Carlo methods are similar to those used to study lattice models in condensed matter physics, with significant differences because of the interactions and because one is often interested in projecting to the fixed number of nucleons ensemble. I will not consider these algorithms further, but the interested reader can read about them in articles by Koonin, Langanke, Dean, Alhassid, and others.[2]

2. Nuclei and Nuclear Interactions

The simplest possible picture of nuclei is as a system of nucleons interacting through two- (and possibly three- or more) body interactions. At high energies and momenta such a picture will certainly fail because of the internal structure of the nucleons. At low and moderate values of momenta and energy, though, this picture can be extremely useful in developing a comprehensive understanding of nuclei and their reactions.

The nucleon-nucleon interaction is extremely well-studied experimentally.[3] Given the large number of experiments and observables in the nucleon-nucleon (NN) sector, it is possible to construct accurate phase-shift analyses of NN scattering. These analyses have been pursued by several groups, and a variety of interaction models have been fit to the phase shifts. The most important feature of the interaction at long distance is the exchange of virtual pions. Pions are charged and couple to the spins of the nucleons, their contribution to the NN interaction can be written:

$$V^{\pi}(r_{ij}) = Y_{\pi}(r_{ij})\sigma_i \cdot \sigma_j + T_{\pi}(r_{ij})\ [3\sigma_i \cdot \hat{r}_{ij}\sigma_j \cdot \hat{r}_{ij} - \sigma_i \cdot \sigma_j\ ], \qquad (1)$$

where σ_i and τ_i are the SU2 Pauli spins and isospins of nucleon i. We use an isospin basis to describe neutrons and protons, neutrons are isospin down states and protons isospin up. Since the Hamiltonian conserves charge, the interaction can only exchange isospins (charge); however the total third component of spin is not conserved and the Hamiltonian flips spins, mixing states of different S_Z.

The functions Y_π and T_π are radial functions in the separations between nucleons i and j, and have the range of an inverse pion mass (μ), or about 1.4 fermi:

$$\begin{aligned} Y_{\pi}(r) &= \exp(-\mu r)/(\mu r) \\ T_{\pi}(r) &= [\ 1 + 3/(\mu r) + 3/(\mu r)^2\ ]\exp(-\mu r)/(\mu r). \end{aligned} \qquad (2)$$

At short distances, the nucleon-nucleon interaction is very repulsive, while at intermediate distances it is attractive. It is the combination of this intermediate range attraction and the correlations invoked by one pion exchange that binds nucleons into nuclei. The most important parts of the NN interaction can be written as a sum of spin-isospin operators times radial functions:

$$V_{ij} = \sum_k V_k(r_{ij})\ O^k(r_{ij}), \qquad (3)$$

where the operators can be taken as a product of spin-dependent and isospin-dependent operators:

$$O^k = [1, \sigma_i \cdot \sigma_j, S_{ij}, L \cdot S_{ij}, L^2,\ L^2 \sigma_i \cdot \sigma_j, L \cdot S_{ij}^2, L \cdot S_{ij}^2 \sigma_i \cdot \sigma_j\ ]\ \times [1, \tau_i \cdot \tau_j], \qquad (4)$$

where L is the relative orbital angular momentum of a pair of nucleons ($L = (r_i - r_j) \times (p_i - p_j)/2$), $L \cdot S$ is the scalar product of the orbital angular momentum and the pair's spin ($S = (\sigma_i + \sigma_j)/2$), and the tensor operator

$$S_{ij} = 3\sigma_i \cdot \hat{r}_{ij}\sigma_j \cdot \hat{r}_{ij} - \sigma_i \cdot \sigma_j. \qquad (5)$$

The exact choice of the operators proportional to the square of the nucleon's momentum (L^2, etc.) depends upon the interaction model.

Beyond the two-nucleon interaction, additional terms are often included in the Hamiltonian. These include relativistic corrections and three-nucleon interactions, which have also been investigated with QMC methods. The three-nucleon interaction can be important because of the relatively low-lying excitations of the nucleon, in particular the Delta resonance. The longest range of the three-nucleon interaction is due to two pion exchanges with the excitation of an intermediate Delta resonance. This force is attractive in light nuclei but repulsive in nuclear matter.[4] Preliminary studies of kinematic relativistic effects, those required by Poincare invariance, indicate a small repulsive effect in light nuclei.[5] Additional terms, those due to the specific nature of the meson-nucleon couplings, are also being investigated in several different formalisms.[6]

3. Nuclear Wave Functions and Spin/Isospin Operators

The wave function of a nucleus can be decomposed into products of spatial amplitudes times spin-isospin states:

$$|\Psi\rangle = \sum_i \phi_i(\mathbf{R})\chi_\sigma\chi_\tau \tag{6}$$

The simplest spin (χ_σ) or isospin (χ_τ) basis is a product of single-particle states with definite z-components of each nucleons spin and isospin. These can be conveniently represented as binary digits[7] which can be combined to represent the A-nucleon spin states as a single integer:

$$\begin{aligned}
\chi_\sigma = \;\; & \downarrow_A\downarrow_{A-1} \cdots \downarrow_2\downarrow_1 && \equiv 0\,0\,0\,0 && = 0 \\
& \downarrow_A\downarrow_{A-1} \cdots \downarrow_2\uparrow_1 && \equiv 0\,0\,0\,1 && = 1 \\
& \downarrow_A\downarrow_{A-1} \cdots \uparrow_2\downarrow_1 && \equiv 0\,0\,1\,0 && = 2 \\
& \downarrow_A\downarrow_{A-1} \cdots \uparrow_2\uparrow_1 && \equiv 0\,0\,1\,1 && = 3 \\
& \quad\vdots && && \\
& \uparrow_A\uparrow_{A-1} \cdots \uparrow_2\uparrow_1 && \equiv 1\,1\,1\,1 && = 2^A - 1
\end{aligned} \tag{7}$$

The isospins can be treated similarly, with $\downarrow$ and $\uparrow$ replaced by n and p, respectively. Charge conservation can be used to limit the number of isospin states used for a given nucleus (there are no four neutron components in ^{4}He). Thus, instead of the wave function being a single function of the 3A coordinates; it is a set of $2^A \times \binom{A}{Z}$ complex functions of the 3A spatial coordinates. Isospin conservation can be used to limit the basis further.

The wave function at a particular set of coordinates is stored as a complex array $\phi(\chi_\sigma, \chi_\tau)$, where the array indices represent the spin-isospin states of the system. The spin indices are given by the integers in the last column of eq. 7. The wave function is described in more detail in the next section, it has a generalized Jastrow form.

In order to construct the wave function or to evaluate the potential energy matrix elements, one must efficiently compute the matrix elements of the two-body spin-isospin operators:

$$O_{ij}^k = [1, \sigma_i \cdot \sigma_j, S_{ij}, L \cdot S_{ij}, ...] \times [1, \tau_i \cdot \tau_j]. \tag{8}$$

The spin operators take a particularly simple form in the basis of definite third components. For example, $\sigma_i \cdot \sigma_j$ is used to describe the difference between spin 0 and spin 1 pairs. In the above basis

$$\sigma_i \cdot \sigma_j = 2P_{ij}^\sigma - 1; \tag{9}$$

where P_{ij}^σ interchanges two spins. Hence acting on a state vector involves only two non-zero matrix elements for each component of the original vector. This basis was originally used by Lomnitz-Adler, Pandharipande, and Smith in [7] and is also covered in the book *Computational Nuclear Physics* by Koonin and Langanke.[8] This chapter also contains a sample Variational Monte Carlo code for 3- and 4-body nuclei that can be quite valuable in reviewing the basic algorithms.

The standard two-body spin-isospin operators are easily recovered using equation 9.

$$\begin{aligned}
\langle\uparrow\uparrow|\sigma_i \cdot \sigma_j|\uparrow\uparrow\rangle &= 1 \\
\langle\downarrow\downarrow|\sigma_i \cdot \sigma_j|\downarrow\downarrow\rangle &= 1 \\
\langle\frac{1}{\sqrt{2}}(\uparrow\downarrow + \downarrow\uparrow)|\sigma_i \cdot \sigma_j|\frac{1}{\sqrt{2}}(\uparrow\downarrow + \downarrow\uparrow)\rangle &= 1 \\
\langle\frac{1}{\sqrt{2}}(\uparrow\downarrow - \downarrow\uparrow)|\sigma_i \cdot \sigma_j|\frac{1}{\sqrt{2}}(\uparrow\downarrow - \downarrow\uparrow)\rangle &= -3.
\end{aligned} \tag{10}$$

Since this spin product exchanges spin but does not flip isolated spins, all off-diagonal matrix elements are zero.

The other spin operators can be handled similarly. A useful relation for the dot product of a spin operator and another vector is:

$$\sigma_i \cdot \mathbf{A} = \sigma_i^+ \mathbf{A}^- + \sigma_i^- \mathbf{A}^+ + \sigma_i^0 \mathbf{A}^0, \tag{11}$$

where we have defined:

$$\sigma_i^+ = \frac{1}{2}(\sigma_i^x + i\sigma_i^y)$$

$$\begin{aligned}
\sigma_i^- &= \frac{1}{2}(\sigma_i^x - i\sigma_i^y) \\
\sigma_i^0 &= \sigma_i^z \\
\mathbf{A}^+ &= (\mathbf{A}^x + i\mathbf{A}^y) \\
\mathbf{A}^- &= (\mathbf{A}^x - i\mathbf{A}^y) \\
\mathbf{A}^0 &= \mathbf{A}^\mathbf{z}
\end{aligned} \tag{12}$$

These (non-standard) spherical tensor operators are also easy to incorporate into our computational scheme. The raising operator σ_i^+ simply flips a spin down nucleon i to spin up up, and gives zero when acting on a state with spin i up. The lowering operator σ_i^- simply reverses this operation, flipping an up spin to down and giving zero when acting on a down spin. Finally, the σ_i^z operator just returns twice the z-component of the spin, +1 for an up spin or -1 for a down spin.

The tensor operator S_{ij} (eq. 5) and the $L \cdot S$ operator, $L \cdot S_{ij} = \mathbf{r}_{ij} \times \mathbf{p}_{ij} \cdot (S_i + S_j)$, can easily be decomposed using the definitions above. The tensor interaction couples spin one pairs with $L = J - 1$ to pairs with $L = J + 1$; it can flip up to two spins at a time. The $L \cdot S$ term flips only one spin at a time as it is linear in the spin. Computing the $L \cdot S$ operator on a state vector requires computing the gradient of the wave function.

We must also consider the isospin dependence of the nuclear interaction. Since the nuclear interaction is predominantly isospin-conserving, the only two-nucleon scalars available are 1 and $\tau_i \cdot \tau_j$. The isospin operator $\tau_i \cdot \tau_j$ is required to describe the difference between pairs of nucleons in isospin one states ($|nn\rangle$, $|pp\rangle$, $|np + pn\rangle$) and isospin zero pairs ($|np - pn\rangle$). Isospin operators can be evaluated explicitly in the complete basis used for the spin states and then transformed into the smaller basis which conserves charge and isospin.

The Coulomb interaction, however, is not isospin-conserving. It is written as

$$V_c(r_{ij}) = \frac{1}{4}\ [1 + \tau_i^z]\ [1 + \tau_j^z]/r_{ij}, \tag{13}$$

where the neutron is a 'down' SU(2) spinor and the proton is an up spinor. For many purposes the Coulomb interaction produces only relatively small effects in light nuclei. Ground state properties are to a good approximation states of good isospin, and high-energy scattering processes are not typically sensitive to the Coulomb interaction. An obvious exception to this rule is the very low-energy reactions that are of astrophysical interest, these will be discussed in a later section. Of course, at very low energies the Coulomb interaction can be extremely important.

4. Variational Wave Functions

We use Variational and Diffusion Monte Carlo methods to calculate the properties of nuclei. To obtain the most accurate energies and observables it is important to have the best possible variational wave functions. Here I briefly describe the wave functions used in present-day calculations and how they are evaluated for a given set of particle coordinates.

Since the nuclear interaction has a strong short-range repulsion, it is natural to use a Jastrow-type wave function. Here, though, the interaction is strongly spin- and isospin-dependent, and hence the correlation functions must be as well. Instead of simple scalar functions of the pair distance, they also depend upon the nucleons spin and isospin configurations. Generically, we can write the wave function as:

$$|\Psi_T\rangle = [\mathcal{S} \prod_{i<j} F_{ij}] \, |\Phi_J\rangle, \tag{14}$$

where the Jastrow state Φ_J contains a product of spin-isospin independent pair correlation functions multiplied by an anti-symmetrized product of single-particle states. $|\Phi_J\rangle$ carries the quantum numbers (J, T) of the state and also much of the long-distance properties of the wave function.

The correlation operators F_{ij} are functions of the pair distance and operators in spin-isospin space. Since they depend upon the spin-isospin states of the nucleons, the different pair operators above do not commute, and we must symmetrize them (indicated by $\mathcal{S}$) by summing over all orders of pair operators. The construction of these correlation operators is described below. For realistic calculations we also use three-nucleon spin-dependent correlations that are explicitly induced by the three-nucleon interaction. For present purposes we ignore this complexity.

The Jastrow state $|\Phi_J\rangle$ must be anti-symmetric in the combined spin-isospin-coordinate space. It is formed by explicitly anti-symmetrizing a product of single-particle states. For the light p-shell nuclei that we are considering, clustering phenomenon can be quite important. One can take the single-particle states as functions of separation from an alpha-particle core. Because of the significantly different average density in the p-shell, it is also useful to take different Jastrow factors for pairs of nucleon in different orbitals.

$$|\Phi_J\rangle = \mathcal{A}[\prod_{ij \in ss, ik \in sp, kl \in pp} f^c_{ss}(r_{ij}) f^c_{sp}(r_{ik}) f^c_{pp}(r_{kl}) |\Phi_0\rangle] \tag{15}$$

The spin-isospin independent correlation functions f^c depend upon the single-particle states of the nucleons: f^c_{ss}, f^c_{sp} and f^c_{pp}, respectively, represent correlations between two s-shell nucleons, and s-shell and a p-shell nucleon, or two p-shell nucleons.

For 3- and 4-particle systems, anti-symmetry can be achieved using only the spin-isospin states. The $|\Phi_0\rangle$ is a pure spin-isospin state with no spatial dependence:

$$\begin{aligned} \Phi_0(^3\mathrm{He}) &= \mathcal{A}|\uparrow p \ \downarrow p \ \uparrow n\rangle \\ \Phi_0(^4\mathrm{He}) &= \mathcal{A}|\uparrow p \ \downarrow p \ \uparrow n \ \downarrow n\rangle \end{aligned} \tag{16}$$

In this case the pair correlation operators f^c_{ss} must decay with the correct asymptotic behavior at large pair separations for a bound state.

For systems of more than 4 nucleons, the Φ_0 must contain a spatial dependence as well. It can be constructed from mean-field like single-particle orbitals $\phi_{l,s}$ taken as a function of the distance from the center of mass of the 4 s-shell nucleons.[4] This preserves many of the important clustering properties in p-shell nuclei. The alpha particle is tightly bound compared to the other nucleons, and it is important to put in this dependence explicitly. Using this clustering property and translational invariance means that the Jastrow wave function is not a simple determinant, and an explicit anti-symmetrization is required. Nevertheless, computing $|\Phi_J\rangle$ is computationally much less demanding than the full calculation of the wave function.

The Jastrow states $|\Phi_J\rangle$ are eigenstates of total (spin plus orbital) angular momentum and total isospin. Since the pair correlation operators described below are translationally invariant and commute with the total angular momentum J, the full wave function is also an eigenstate of both total momentum and total angular momentum.

The pair correlation operators must describe correctly the short-distance physics. They are functions of the pair distances and the most important operators in the interaction:

$$F_{ij} = \sum_k f^k(r_{ij}; \mathbf{R}) O^k_{ij}, \tag{17}$$

where

$$O^k = [1, \sigma_i \cdot \sigma_j, S_{ij}] \times [1, \tau_i \cdot \tau_j]. \tag{18}$$

The pair correlation operators are obtained by solving several two-nucleon Schroedinger-like differential equations with the full two-nucleon interaction plus an added potential $\lambda(r)$. In the singlet (pair spin equal 0) channels this is a simple uncoupled equation:

$$-\hbar^2/(2\mu)\nabla^2[f^{ST}_{ij}\phi_{ij}] + (v_{S=0,T}(r) + \lambda(r))[f^{ST}_{ij}\phi_{ij}] = 0, \tag{19}$$

while in the triplet channels it is a set of two coupled equations. In this equation $\phi(r)$ is the correlation introduced by the single-particle states

$|\Phi_0\rangle$, $\phi = 1$ in even parity channels and $\phi \propto r$ in odd parity channels. After solving for the $f^{ST}(r)$ in different spin-isospin channels, they can be recast into the operator form of equation 18. The parameters in the 'potential' $\lambda(r)$ and the asymptotic boundary conditions used for F_{ij} are treated as variational parameters.

Since the average spin-isospin independent correlation is included in $|\Phi_J\rangle$, the average spin-independent pair correlation f^c is divided out to obtain the spin-isospin dependent correlations:

$$\begin{aligned} f^c(r_{ij})\ F_{ij} &= f^c(r_{ij})[1 + \sum_{k=2} u^k(r_{ij};\mathbf{R})\ O^k_{ij}], \\ F_{ij} &= [1 + U_{ij}] \end{aligned} \tag{20}$$

The functions u^k are ratios of the non-central to central correlation functions.

There is a frustration induced by the different pair potentials (not all pairs can be simultaneously diagonalized), and hence there is a quenching of the spin-isospin pair correlation operators due to the presence of the other particles. This quenching is parameterized as an extra dependence of the 'pair' correlation operators U_{ij} on the coordinates of the other particles $\mathbf{R}$. Hence while F_{ij} depends upon the spins and isospins only of particles i and j, it depends upon the coordinates of all the particles.

Thus, the full variational wave function is:

$$|\Psi_T\rangle \quad = \quad \mathcal{S} \prod_{i<j}[1 + U_{ij}]\ |\Phi_J\rangle \tag{21}$$

It contains approximately 20-30 variational parameters, parameters in the pair correlations which govern the short-range correlations, and parameters in the $\Phi_0\rangle$ which governs the long-distance properties.

5. Variational Monte Carlo

Given a form of variational wave function, the parameters in the wave function must be optimized in a Variational Monte Carlo calculation. Once choice is to minimize the variational energy. The Monte Carlo scheme here is rather similar to a standard calculation with state-independent interactions. Metropolis Monte Carlo methods are used to perform the spatial integrals, while the spin-isospin sums are evaluated explicitly. The state dependence of the interaction does introduce some additional complexity into the algorithm, however.

For example, in addition to the spatial integrals, it is also advantageous to sample the sums over orders of pair correlation operators implied by $\mathcal{S}$ in the wave function (eq. 21). It would be computationally very expensive to sum over all $(N(N-1)/2)!$ pair orderings (or even the subset of distinct orderings of non-commuting operators), and hence we simply choose random orders $(o_l,\ o_r)$ of operators independently for the left and right-hand wave functions. The left and right-hand wave functions are then denoted as Ψ_l and Ψ_r, respectively. These wave functions are identical when summed over all pair orderings, but are not identical for a specific o_l, o_r.

Calculating the wave function for a given set of particle positions then involves the following steps:
(1) Calculate the single particle orbitals $\phi_{l,s}$ for each nucleon and each possible clustering of nucleons into s- and p-wave states.
(2) Combine these single particle orbitals into the Φ_J by forming products of allowed single-particle states (e.g. 4 s-shell nucleons and 2 p-shell nucleons for ^{6}Li). Each product of single particle orbitals must be multiplied by the product of central correlations f^c. The products are then combined into the explicitly anti-symmetric Φ_J by summing over allowed permutations with a factor of $(-1)^P$.
(3) Take this single-particle wave function and multiply by the pair correlation operators $1+U_{ij}$ in the specific order given by o_l and o_r, respectively for the left and right hand wave functions.

The first task in a Metropolis Monte Carlo scheme is to define a sampling probability for the Metropolis integration. This sampling probability depends both upon the 3A coordinates R and the orderings (o_l, o_r) of correlation operators on the left and right-hand wave function. A simple choice is:

$$\begin{aligned} W(R) &= \sum_i |\ \mathrm{Re}\langle\Psi_l|\chi_\sigma(i)\chi_\tau(i)\rangle\langle\chi_\sigma(i)\chi_\tau(i)|\Psi_r\rangle| \\ &+ \ \epsilon\ |\langle\Psi_l|\chi_\sigma(i)\chi_\tau(i)\rangle\langle\chi_\sigma(i)\chi_\tau(i)|\Psi_r\rangle|, \end{aligned} \tag{22}$$

where the sums run over all spin-isospin states of the system. The second terms assures (for small positive epsilon) that the probability density W(R) is positive definite. This term is required since Ψ_l and Ψ_r are not Hermitian conjugates (different specific pair orderings have been chosen for each). The sampling over pair orders has introduced some additional complexity, and potentially significant additional fluctuations. In practice, however, these fluctuations are relatively small compared to the other errors in the variational wave function and it is far more efficient to sample the pair orders than to completely evaluate them.

The Metropolis Monte Carlo calculation proceeds in the standard way, accepting or rejecting moves based upon the value of W(R) at the proposed and last accepted points. Once the asymptotic distribution has been reached, a set of points can been obtained with probability density proportional to $W(R)$. Summing over these points leads to the standard expressions for matrix elements

$$\langle O \rangle = \frac{\sum_j \langle \Psi_l(R_j) | O | \Psi_r(R_j) \rangle / W(R_j)}{\sum_j \langle \Psi_l(R_j) | \Psi_r(R_j) \rangle / W(R_j)}, \tag{23}$$

where the angled brackets indicate an implicit sum over all spin-isospin states for each configuration. The optimum variational wave function is obtained by minimizing the energy. The standard technique of calculating energy differences is extremely useful for this optimization. It is also possible to minimize the variance in the calculation of the energy. However, even if the full variational wave function were an exact eigenstate of the Hamiltonian, sampling over the pair orders would introduce a finite variance into a calculation of the energy and hence we cannot expect a zero variance solution.

For nuclei with A=6-8, the variational procedure outlined above has not yet been successful in producing binding compared to the lowest available breakup thresholds. Presumably there is some significant three-body correlation that is missing in the variational wave function. Since we are interested in using these wave functions as input to Diffusion Monte Carlo calculations, it is valuable to constrain the variational wave functions to have approximately the correct experimental charge radius. As the DMC calculations do produce binding, this is a natural way to maximize the overlap of the variational and true ground-state solutions.

In the above, we have simplified several aspects of the calculations. For example, three-nucleon correlations are important, and must be included in the variational wave function. These are written as $F_{ijk} = 1 - \beta \tilde{V}_{ijk}$, where β is a variational parameter and $\tilde{V}_{ijk}$ indicates a three-nucleon interaction where the distances have been multiplied by a scale factor. In the Monte Carlo, one again introduces a sampling order for the triplets in the three-body correlations.

Also, we have been assuming up to now that there is a unique combination of low-lying single particle orbitals that can yield a given set of quantum numbers. In reality, for A=6-8 the Jastrow state Φ_J can actually have several different symmetry components. It is possible to combine several p-wave nucleons in different ways (different m-states in angular momentum, spin, and isospin) to produce the same total quantum numbers J^π, T. Cohen and Kurath[9] showed using the shell model that the dominant long-distance component of the wave function is the most spatially symmetric one. Rather than simply assuming that, we diagonalize the Hamiltonian in this basis of possible shell-model orbitals. We typically find small 10-20 per cent admixtures of other symmetry states in the full wave function. It is important to include this affect at the variational level because it is very difficult to use Diffusion Monte Carlo to project out the true ground state otherwise. These long-wavelength modes are very low energy excitations (a few MeV) and are difficult to treat due to the fermion sign problem in the DMC calculation. We are presently checking the accuracy of doing this diagonalization at the VMC level by computing matrix elements in the DMC calculations.

In addition to energies, a variety of other experimental observables are readily calculated. These include electromagnetic form factors (elastic and transition), momentum distributions, quadrupole moments, asymptotic normalizations, etc. These are either directly or indirectly accessible through electron scattering measurements. In general, these calculations give impressive agreement with experiment. We also wish to calculate low-energy reactions and the nuclear response directly, these can also be done with QMC methods, as will be discussed in later sections. First, though, we turn to Diffusion or Green's function Monte Carlo studies of nuclear bound states.

6. Diffusion or Green's function Monte Carlo

Diffusion or Green's function Monte Carlo are often used to improve the wave function and energy obtained in VMC calculations. Nuclear physics is no exception; indeed, some of the earliest applications of QMC methods were to problems in nuclear physics (the alpha particle or idealized neutron matter). These early applications used spin-isospin averaged central interactions, however, so the results were not tied directly to NN interactions.

In order to use Quantum Monte Carlo methods to solve for properties of nuclei, one must generalize the algorithms commonly used for spin-independent interactions. In principle this is straightforward, as we simply want to use Monte Carlo methods to evaluate integrals of the type:

$$\langle \Psi_T | O | \Psi(\tau) \rangle = \langle \Psi_T | \ O \prod_{i=1,N} \exp[-H\Delta\tau] \ | \ \Psi_T \rangle > . \tag{24}$$

First we discuss the calculation of the propagator matrix elements, and then the sampling of the paths.

It is useful to write the imaginary time propagator as a (symmetrized) product of two-body propagators:

$$\langle \mathbf{R}', \chi' | \exp(-H\Delta\tau) | \mathbf{R}, \chi \rangle \equiv G(\mathbf{R}', \mathbf{R}; \Delta\tau) \approx \left[\prod_{i=1,A} G_{0,i}(|\mathbf{r}_i - \mathbf{r}'_i|) \right]$$
$$\times \sum_{\chi_1,\chi_2} \langle \chi' | \left[1 - \frac{\Delta\tau}{2} \sum_{i<j<k} V_{ijk}(\mathbf{R}') \right] |\chi_1\rangle \langle \chi_1 | \mathcal{S} \prod_{i<j} \left[\frac{g_{ij}(\mathbf{r}'_{ij}, \mathbf{r}_{ij})}{g_{0,ij}(\mathbf{r}'_{ij}, \mathbf{r}_{ij})} \right] |\chi_2\rangle$$

$$\times\langle\chi_2|\left[1-\frac{\Delta\tau}{2}\sum_{i<j<k}V_{ijk}(\mathbf{R})\right]|\chi\rangle, \quad (25)$$

where the χ represent A-nucleon spin-isospin states, $G_{0,i}$ and $g_{0,ij}$ are the free one- and two-body imaginary-time propagators, respectively, and g_{ij} is the interacting two-body propagator.

The free propagators are simple Gaussians:

$$G_{0,i} = N_1 \exp\left[-m\frac{(\mathbf{r}_i'-\mathbf{r}_i)^2}{2\Delta\tau}\right] \quad , \quad (26)$$

$$g_{0,ij} = N_2 \exp\left[-m\frac{(\mathbf{r}_{ij}'-\mathbf{r}_{ij})^2}{4\Delta\tau}\right] \quad , \quad (27)$$

with normalizations N_i such that the norm of the flux is preserved ($\int d\mathbf{r}_i\, G_{0,i} = 1$). The pair propagator g_{ij} is the imaginary-time equivalent of the two-body T matrix, it is a matrix in the two-body spin-isospin space and must be calculated numerically. The propagator satisfies an evolution equation:

$$\langle\chi_{ij}'|\left[\frac{\partial}{\partial\tau}+H_{ij}\right] g_{ij}(\mathbf{r}',\mathbf{r};\tau)|\chi_{ij}\rangle = 0 \quad , \quad (28)$$

where

$$H_{ij} = -(1/m)\nabla_{ij}^2 + v_{ij} \quad , \quad (29)$$

and χ_{ij} and χ_{ij}' are two-nucleon spin-isospin states. The g_{ij} also satisfy a boundary condition

$$\langle\chi_{ij}'|g_{ij}(\mathbf{r}',\mathbf{r};\tau{=}0)|\chi_{ij}\rangle = \delta(\mathbf{r}-\mathbf{r}')\delta_{\chi_{ij}',\chi_{ij}}. \quad (30)$$

The techniques for calculating and storing g_{ij} are described in detail in the paper by Pudliner, et al.[4] While they are basically the same as for standard interactions, the coupling of spins to space means that the pair propagators are calculated in partial waves which couple L and S to good total J. Evaluating the pair propagator for a given set of initial and final states involves rotating SU2 states from initial points along $\hat{z}$ and final points in the $x-z$ plane, where the matrices are stored, to the actual initial and final coordinates.

The first calculations were actually performed with the simpler primitive propagator $G = \exp[-V\Delta\tau/2]\ \exp[-T\Delta\tau]\ \exp[-V\Delta\tau/2]$; although this is less efficient it is useful to help understand how the algorithm works. The pair potential can be diagonalized by working in states of good total spin and isospin. In the spin zero channels the potential is then just a number and can be easily exponentiated. In the spin one channels the static part of the potential can be re-written in the form

$$V_{S=1,T} = \tilde{v}_c + \tilde{v}_t \sigma_i \cdot \hat{r}_{ij} \ \sigma_j \cdot \hat{r}_{ij}. \tag{31}$$

Since $[\sigma_i \cdot \hat{r}_{ij} \ \sigma_j \cdot \hat{r}_{ij}]^2 = 1$, this part of the potential can also be easily exponentiated. The different channels can then be combined back to ordinary operator products, and the propagator put in a form very similar to that used for the pair correlation operator in the variational wave function (Eq. 18). Since the potential enters the propagator at order $\Delta\tau$, the spin-isospin rotations induced are relatively slow and do not cause excessive difficulties in the Monte Carlo sampling. Terms proportional to $L \cdot S$ also enter the potential, at the level of the primitive propagator these can be obtained by letting the momentum operator act on the free-particle propagator and symmetrizing between initial and final points. The spin can be though of as defining an axis, and the $L \cdot S$ operator differentiates between positive and negative rotations about that axis. This introduces a phase factor $e^{i\phi}$ which depends upon the vector triple product of the pair separation, the orientation of the nucleons spins, and the direction of the step in imaginary time. Since we always sum over all orientations of the spins, we are summing phases which cancel to some extent, and this does not introduce as much statistical error as one might naively think. The higher-order momentum dependent operators are more difficult; they essentially involve different effective-mass terms in different spin-isospin states. To date, these relatively small terms have been handled perturbatively.

Once the propagator $G(\mathbf{R}, \mathbf{R}'; \Delta\tau)$ is constructed, a practical algorithm must be implemented to carry out the iteration of the wave function, eq. (24). The scheme currently used for sampling the paths is described in detail in reference [4], here we simply sketch the basic ideas. Since the wave function (propagators) are vectors (matrices) in spin-isospin space, a scalar quantity must be defined to sample the paths. In principle, any set of paths can be chosen as long as the probability used to choose the paths is divided out when computing expectation values. To minimize the variance, though, it is important to follow as closely as possible standard importance sampling techniques used in traditional Green's function and Diffusion Monte Carlo. In essence, this requires sampling from a kernel so that the probability of a configuration at $\mathbf{R}$ is proportional to $\sum_\chi \langle \Psi_T(\mathbf{R})|\chi\rangle\langle\chi|\Psi(\mathbf{R};\tau)\rangle$. In the limit that the trial wave function Ψ_T is exact, and the propagator is sampled exactly, this method would produce the correct ground-state energy with no variance.

To this end, we use an importance function I that is the analogue of the weight function W used in VMC calculations. The importance function is a function of all the spin-isospin components in the full trial and

GFMC wave functions. The calculations proceed by sampling paths from $I[\Psi_T(\mathbf{R}'), \Psi(\mathbf{R}'; \tau)]$, The importance function must be real and positive, a convenient choice is:

$$\begin{aligned} I[\Psi_T(\mathbf{R}), \Psi(\mathbf{R})] &= |\mathrm{Re} \sum_\chi \langle \Psi_T(\mathbf{R}) | \chi \rangle \langle \chi | \Psi(\mathbf{R}; \tau) \rangle | \\ &+ \epsilon \sum_\chi | \langle \Psi_T(\mathbf{R}) | \chi \rangle \langle \chi | \Psi(\mathbf{R}; \tau) \rangle | \ , \end{aligned} \tag{32}$$

where ϵ is again a small positive coefficient. The second term ensures that all paths are allowed with a positive probability. In this equation and those that follow, the dependence upon the symmetrization $\mathcal{S}$ in the pair and triplet orders will be suppressed, both in the wave function, eq. (21), and the propagator, eq. (25). The pair and triplet orders are, in fact, sampled in both cases. Details of the sampling and weighting of paths are described in Pudliner, et al.[4]

Computationally, it would be extremely costly to compute the derivative of the full wave function in order to implement importance sampling. Instead, we use an intermediate approximate importance sampling based upon a spin-isospin independent function to calculate 6N possible next steps (6N orthogonal steps along +/- directions on randomly oriented axes). This is very quick since we are dealing with only spin-isospin independent quantities. We then choose one actual next step from these 6N steps and calculate the full propagation, dividing out the effects of this approximate importance sampling. This allows us to compute a step relatively quickly (no derivatives and only one set of pair propagators acting on the full wave function) while retaining, to a large extent, the low-variance properties of importance sampling.

Branching techniques are used to split (delete) paths with large (small) importance functions $I[\Psi_T(\mathbf{R}'), \Psi(\mathbf{R}'; \tau)]$ in a statistically unbiased manner. After branching, expectation values can be recovered from the operator evaluated between the trial and propagated GFMC wave functions:

$$\langle O(\tau) \rangle \approx \frac{\sum_i \langle \Psi_T(\mathbf{R}_i) | O | \Psi(\mathbf{R}_i; \tau) \rangle / I[\Psi_T(\mathbf{R}_i), \Psi(\mathbf{R}_i; \tau)]}{\sum_i \langle \Psi_T(\mathbf{R}_i) | \Psi(\mathbf{R}_i; \tau) \rangle / I[\Psi_T(\mathbf{R}_i), \Psi(\mathbf{R}_i; \tau)]} \ . \tag{33}$$

This is the basis of the importance sampled GFMC algorithm for non-central interactions. Iterating this equation propagates the amplitudes of the wave function in a way designed to minimize statistical fluctuations in calculated expectation values.

The matrix element in eq. (33) is a "mixed" estimate; it is of the form

$$\langle O \rangle_{\mathrm{mix}} = \frac{\langle \Psi_T | O \exp(-H\tau) | \Psi_T \rangle}{\langle \Psi_T | \exp(-H\tau) | \Psi_T \rangle} \ . \tag{34}$$

The value O_{mix} is the matrix element of the trial (variational) and the true ground state. The mixed estimate is sufficient to evaluate the ground state energy, since the Hamiltonian commutes with the propagator. Indeed, an upper bound to the true ground-state energy E_0 is obtained for any value of τ:

$$\langle H \rangle_{\text{mix}} = \frac{\langle \Psi_T | \exp(-H\tau/2) H \exp(-H\tau/2) | \Psi_T \rangle}{\langle \Psi_T | \exp(-H\tau/2) \exp(-H\tau/2) | \Psi_T \rangle} \geq E_0 \quad . \tag{35}$$

Of course, the actual convergence is governed by the accuracy of the trial wave function and the spectrum of the Hamiltonian. Often knowledge of the spectrum can be used to estimate the remaining error in a calculation that necessarily proceeds to only a finite τ.

For quantities other than the energy, one typically estimates the true ground-state expectation value by extrapolating from the mixed and variational estimates:

$$\langle O \rangle \approx 2 \, \langle O \rangle_{\text{mix}} - \frac{\langle \Psi_T | O | \Psi_T \rangle}{\langle \Psi_T | \Psi_T \rangle} \quad , \tag{36}$$

which is accurate to first order in the difference between Ψ and Ψ_T. The variational wave functions used in this work are typically quite accurate, so this estimate is usually sufficient. For momentum-independent quantities, one can also retain a time history of the path in order to reconstruct an estimate of the form:

$$\langle O \rangle = \frac{\langle \Psi_T | \exp(-H\tau/2) O \exp(-H\tau/2) | \Psi_T \rangle}{\langle \Psi_T | \exp(-H\tau/2) \exp(-H\tau/2) | \Psi_T \rangle} \quad . \tag{37}$$

GFMC has proven to be quite accurate in the three, and now four, body systems in which it has been tested. Recent applications to larger systems provide the first real tests of these microscopic models beyond A=4.[4] Figure 1 displays the present-day results of realistic nuclear interaction models. The overall agreement between theory and experiment is very satisfying. The absolute energies are reproduced within a few MeV or less whereas the interaction energies are on the order of several hundred MeV. The low-lying excitations are also well-reproduced, with the correct ordering of the spectra.

Remaining discrepancies are on the order of a few MeV, which is smaller than the scale of the three-nucleon interaction and relativistic effects. In particular the isospin-rich nuclei are lie too high in energy, and the $L \cdot S$ splittings are smaller than experiment. Present-day crude models of relativistic and three-nucleon interaction effects need to be improved in order to reproduce the spectra more precisely. While this fine adjustment is not necessary to understand the bulk properties of nuclei, it is important when

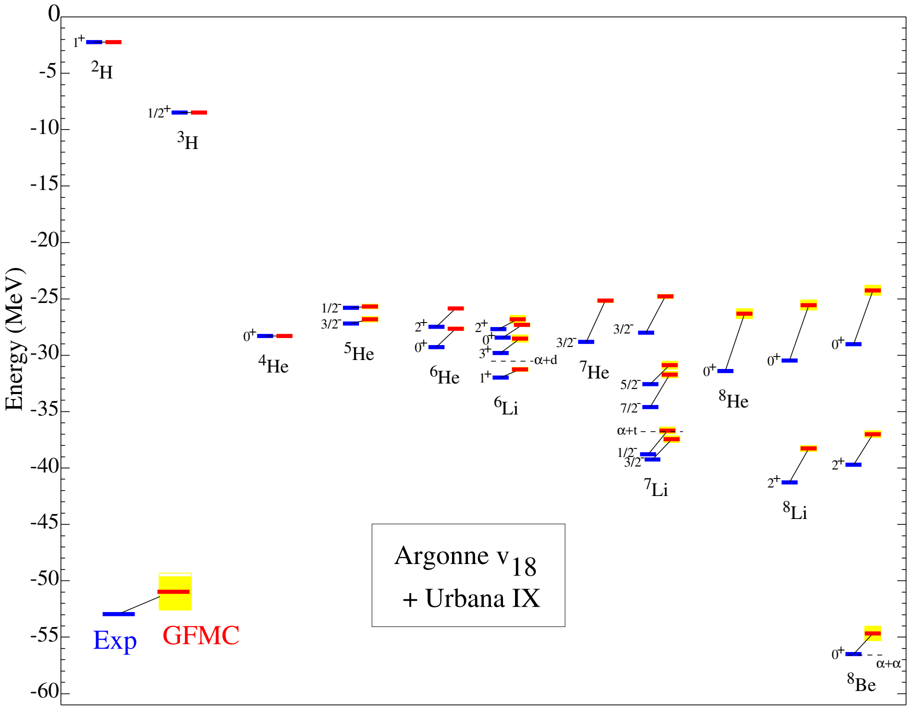

Figure 1. Comparisons of experimental light nuclear spectra with quantum Monte Carlo calculations. Spin-parity assignments are listed for each state. Results shown are obtained from transient estimation; one sigma error bars are indicated by light shaded regions.

attempting to extend studies to neutron rich nuclei or neutron star matter or to get the correct thresholds for low-energy scattering. These projects are important lines of future study. The former can be studied with traditional bound-state methods; applications to low-energy scattering will be discussed in the next section.

7. Low Energy Reactions – Methods and Applications

A variety of important nuclear reactions occur at very low energies, including the fusion reactions that are the source of solar neutrinos. Reaction rates for neutrino production in the sun can be very difficult to measure because of the required penetration of the Coulomb barrier at extremely low energies. A variety of other experiments are also performed at low energies, these can both improve our understanding of nuclei and the role of fundamental interactions in the nucleus. These experiments include studies of electromagnetic capture rates and tests of the weak parity-violating (PV) nucleon-nucleon interaction.

While, except for very small systems, there exists no general method for calculating of quantum scattering, reactions at low energy are a special case and can be treated with Quantum Monte Carlo methods. Low-energy here implies an energy such that only one (or at most a few) possible break-up channels are available. The necessity of this restriction will be obvious when discussing the method. Before proceeding to method, though, one should note that it is also possible to use QMC to gain information about the other extreme of quantum scattering, extremely high-energy scattering. Here semi-classical methods such as Glauber theory are very valuable, and QMC can be used to test and refine such schemes.[10]

At low energies, we first consider the scattering wave function in the limit as two clusters separate. Generically, we may express the wave function as

$$\Psi = \psi_1 \times \psi_2 \times \phi_{rel}(R_1 - R_2), \tag{38}$$

where ψ_1 and ψ_2 are the internal wave functions of clusters 1 and 2, respectively, and ϕ_{rel} is the wave function in the relative coordinates between the center of mass of the two clusters. In the general case with spin, the asymptotic wave function will be a linear combination of terms coupled to good total angular momentum J. Here we discuss the simpler case without spin.

If only one scattering channel is energetically allowed, the relative wave function can be decomposed in a simple way into different partial waves. The asymptotic wave function in a partial wave of angular momentum L is proportional to

$$\phi_{rel}(R_1 - R_2) = P_L(\Omega_{12})\phi(|R_{12}|), \tag{39}$$

and

$$\phi(|R_{12}|) \propto \cos(\delta_L(E))\ j_L(kR) - \sin(\delta_L(E))\ n_L(kR). \tag{40}$$

This separation into partial waves is crucial to performing a QMC calculation. The time-independent scattering states in each partial wave are stationary states with no flux into or out of the reaction region, and hence the radial part of the relative wave function can be taken purely real. Also, the asymptotic normalization of the wave function is not relevant for computing the phase shift, just as in the bound state problem.

To obtain the phase shift, we confine the system to a region where the magnitude of relative coordinate $|R_{12}| \leq R_b$. The confining or 'box' radius R_b must be large enough so that the two constituent clusters do not interact, and hence the above form of the relative wave function is valid. In the case of charged clusters, the Coulomb functions must be used in place of the spherical Bessel functions. Calculations are performed within a region where R_b is as small as possible consistent with the requirement of non-interacting (or only Coulomb forces) between clusters. At the boundary

$|R_{12}| = R_b$ we enforce a boundary condition on the wave function

$$\left. \frac{\hat{S} \cdot \nabla_{R_{12}} \Psi}{\Psi} \right|_{R_{12}=R_b} = \beta. \tag{41}$$

The constant β can be adjusted as desired. For each, or possibly for many, values of β we use standard MC methods to solve for the low-lying states of the system. If there is a bound state in the system, the radius R_b must be such that this bound state is entirely contained within R_b. In exceptional cases this can be a more stringent requirement than that of non-interacting clusters, but typically this is not the case. For cases with bound states, it is necessary to orthogonalize the scattering states to the ground state.

For each state with a total energy E greater than the energy of the two clusters $E_1 + E_2$, we can attach an asymptotic scattering state of energy $E_{scat} = E - (E_1 + E_2)$ and momentum $k = \sqrt{(2\mu E_{scat}/\hbar^2)}$, where μ is the reduced mass of the two clusters. The scattering wave function can be attached smoothly to the solution within the scattering region and the scattering phase shift δ_L obtained from the asymptotic form of the logarithmic derivative of the wave function (eq. 40). Instead of assuming E and solving for the scattering state, we assume a boundary condition and find E_{scat} and hence $\delta_L(E_{scat})$.

Instead of setting the logarithmic derivative, it is also possible to enforce a node of the wave function at a radius R_b. This has been done, for example, in VMC studies of excitations in the alpha particle.[11] Either boundary condition is easy to implement in a Diffusion or Green's function Monte Carlo scheme. The boundary condition supplies the necessary information for introducing image points outside the radius R_b whose contributions in the next generation must be included. One way to do this is for each R set a new point R_{img} along $\hat{R}$ such that $R \cdot R_{img} = R_b^2$. The relative contribution of points from R_{img} can be easily added to those from R in the DMC scheme. It should be emphasized that either form of boundary condition is not an approximation; it is exact given a method for solving for the internal wave function exactly.

This method is variational in the sense of being second order in the difference between the true and exact wave function, since the standard stationary variational principles apply. It also provides an upper bound principle for the energy with a specific boundary condition. In a Monte Carlo calculation it is very helpful to have an upper bound principle at the level of calculating the energy. In standard scattering calculations, the Kohn variational principle is typically used, which is a stationary principle rather than a bound.

It is useful to consider two typical cases for scattering states at low energy. First consider zero-energy scattering, where we would like to calculate the scattering length. This can be obtained by adjusting the logarithmic derivative until $E_{scat} = 0$ is obtained. The scattering length is just given by extending the asymptotic linear wave function to the zero intercept. The effective range would be given by the derivative of the energy with respect to the change in the boundary condition. Energy-difference techniques can be used to locate the boundary condition for which $E_{scat} = 0$. It is possible to obtain unphysical boundary conditions which would imply exponentially growing asymptotic wave functions. However, these unphysical states can always be discarded by adjusting the boundary condition appropriately.

Another typical process of interest is determining properties of a resonant state. A typical resonance, in this picture, will occur when we have an 'almost-bound' state. Here the wave function will be largely contained well within the interior of the scattering region, and hence the energy will be display very little sensitivity to the boundary condition. Again, energy differences will be required to determine the location and especially the width of the resonance.

We have employed these techniques in a variety of interesting physical settings, including the excited states of the alpha particle, the strong-interaction phases of proton-alpha and neutron-alpha scattering,[12] the weak and EM capture processes in A=4,[13, 14] and parity violation in the low-energy scattering of neutrons by Helium. The weak capture in A=4 is very interesting in terms of the recent results from SuperKamiokande,[15] and the PV measurements of neutron scattering from Helium-4 will tell us much about the parity violating weak coupling of pions to nucleons.

8. Nuclear Correlations and Response

The nucleon-nucleon interaction is quite repulsive at short distances and hence is expected to induce strong correlations between nucleons at pair separations on the order of 1 fermi. An interesting question is to what extent these correlations can be measured in nuclei. Experimental tools at our disposal include electron scattering experiments as well as hadronic probes. More generally, we would like to understand not only the ground state correlations in the nucleus, but also the response of nuclei to electromagnetic and hadronic probes.

The total cross section of electrons scattered by nuclei can be expressed as the sum of two terms, a longitudinal (charge) response and a transverse (current) response.

$$\frac{d^2\sigma}{d\omega\, d\Omega} = \sigma_M \left[v_L R_L(\mathbf{q}, \omega) + v_T R_T(\mathbf{q}, \omega) \right] \,, \tag{42}$$

where σ_M is the standard Mott cross section, and v_L and v_T are kinematical factors depending upon momentum- and energy-transfer. The longitudinal

(R_L) and transverse (R_T) response are the experimental quantities which we wish to understand. These can be separated experimentally by performing experiments with the same energy and momentum transfer to the nucleus, but with different electron scattering angles, and hence different v_L and v_T.

The longitudinal response is governed by the nuclear charge operator, given approximately by

$$\rho_L(q) = \sum_i \frac{1+\tau_i^z}{2} \exp[iq \cdot r] G_E^p(q), \tag{43}$$

which is just a plane wave for the electron multiplied by a proton projection operator and the electric (charge) form factor of the proton evaluated at a momentum q. Corrections to this formula occur because of the relatively small charge form factor of the neutron plus small relativistic effects.

The longitudinal or charge response is

$$S_L(q,\omega) = \sum_f \langle 0|\rho_L^\dagger(q)|f\rangle\langle f|\rho_L(q)|0\rangle\delta(\omega - (E_f - E_0)). \tag{44}$$

The Coulomb sum rule is obtained by dividing out the proton form factors and integrating over the energy loss to obtain ω to obtain

$$S_{pp}(q) = Z + \frac{Z(Z-1)}{2}\rho_{pp}(q), \tag{45}$$

where Z is the number of protons in the nucleus and $\rho_{pp}(q)$ is the Fourier Bessel transform of the proton-proton correlation function. Hence the integrated longitudinal response of nuclei contains information on the correlations of protons in the nucleus. Experimental and theoretical studies of this response have confirmed the presence of a strong short-range repulsion between protons in ^{3}He and ^{4}He.[16] Experiments in larger nuclei are not consistent, however,[17] and should be reexamined.

It is more difficult to provide a direct measure of the spin-space tensor correlations between nucleons. Two reactions are, in principle, sensitive to correlations between np pairs in the nucleus. In the Bethe-Levinger picture, the total absorption cross section for pions or photons is proportional to the number of quasi-deuteron np pairs in the nucleus. Qualitatively a consistent picture of these reactions is found up to the largest nuclei where microscopic calculations have been undertaken, ^{1}6O.[18] More refined conclusions are not yet possible, however.

We can also gain information on nuclear dynamics by examining the imaginary-time response in the nucleus. This response is defined as

$$\begin{aligned} S(q,\tau) &= \int d\omega \exp[-H\tau] S(q,\omega) \\ &= \langle 0|\ \rho^\dagger(q)\ \exp[-H\tau]\ \rho(q)\ |0\rangle. \end{aligned} \tag{46}$$

This is very similar to calculations of zero-temperature imaginary time response in condensed matter physics. For the longitudinal response, though, the operator couples to the nuclear charge density as opposed to the baryonic density. This is an important distinction, because the Hamiltonian does not commute with the coupling ρ_L. The interaction propagates charge through the one-pion-exchange interaction, for example. Hence in this non-relativistic approximation charge is instaneously propagated over distances of the order of an inverse pion mass. Rewriting the imaginary-time response in terms of coherent and incoherent scattering,

$$\begin{aligned} S_L(q,\tau) &= \sum_{i\neq j} \langle 0|\rho_L^\dagger(i)\exp[-H\tau]\rho_L(j)|0\rangle\rangle \\ &+ \sum_i \langle 0|\rho_L^\dagger(i)\exp[-H\tau]\rho_L(i)|0\rangle\rangle \end{aligned} \tag{47}$$

The second term is most important in the quasi-elastic scattering regime where the dominant scattering amplitude is from one nucleon at a time. This is mostly true at larger momentum transfers and higher energies, which corresponds to shorter imaginary time. At large imaginary time, both terms are important as we are dealing with scattering off the whole nucleus.

At $\tau = 0$, the longitudinal response $S_L(q,\tau)$ corresponds to the Coulomb sum rule, and derivatives with respect to τ correspond to energy-weighted sum rules. In the regime where incoherent scattering dominates (the second term of eq. 47), we can think of electron scattering from a proton i. The proton propagates in imaginary time, and if we consider only the momentum distribution or spectral function of the initial proton we will obtain the standard expressions for the plane-wave-impulse-approximation response.[1] However, final-state interactions are also important. In particular, for finite tau, the interaction can exchange charge between nucleons. In sum rule terms, this means that the energy-weighted sum rule of the longitudinal response will be larger than $q^2/2m$. In the imaginary-time propagation, this will manifest itself as a more rapid decrease with τ in the incoherent scattering contribution to the response. This interaction effect can produce dramatically different response functions for different probes of the nucleus.

The response of the alpha particle to different idealized probes are presented in Figure 2. These idealized probes are:

$$\rho_N(\mathbf{q}) = \sum_i e^{i\mathbf{q}\cdot\mathbf{r}_i} \ , \tag{48}$$

$$\rho_p(\mathbf{q}) = \sum_i e^{i\mathbf{q}\cdot\mathbf{r}_i} \ \frac{1+\tau_{z,i}}{2} \ , \tag{49}$$

$$\rho_\tau(\mathbf{q}) = \sum_i e^{i\mathbf{q}\cdot\mathbf{r}_i} \ \tau_{+,i} \ , \tag{50}$$

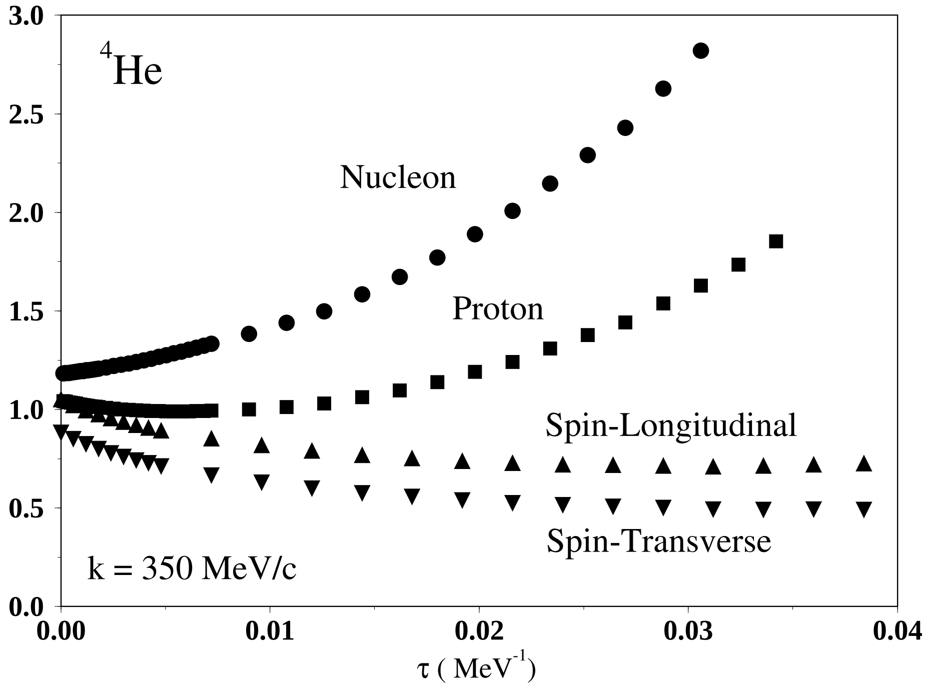

Figure 2. Response of the alpha particle to various idealized single-nucleon couplings (see text). The response has been multiplied by a scale factor of $\exp(q^2 \tau / 2m)$ for clarity, with this scaling the response of an isolated nucleon would have a constant value of one.

$$\rho_{\sigma\tau L}(\mathbf{q}) = \sum_i e^{i\mathbf{q}\cdot\mathbf{r}_i} (\sigma_i \cdot \hat{\mathbf{q}})\ \tau_{+,i}\ , \tag{51}$$

$$\rho_{\sigma\tau T}(\mathbf{q}) = \sum_i e^{i\mathbf{q}\cdot\mathbf{r}_i} (\sigma_i \times \hat{\mathbf{q}})\ \tau_{+,i}\ , \tag{52}$$

and represent the nucleon, proton, isovector, spin-longitudinal, and spin-transverse couplings, respectively. Note that the isovector ($\propto \tau_z(i)$) couplings are dramatically reduced at low τ, corresponding to an increase in the energy-weighted sum rules. At large τ, which corresponds to low excitation energies, the responses are also dramatically different. The nature of the low-energy response depends very much upon the nucleus and its low-lying excitation spectrum. In the alpha particle, the lowest excitations are nearly 20 MeV, so probes which couple back to the elastic ground-state channel are much enhanced at large tau. One important issue in QMC calculations of the response is how best to calculate the response to specific low-lying excited states. Such calculations can be attempted either with imaginary-time response formalism or explicit calculations of the excited states, or in a combined fashion.

For direct comparison with measurements of the longitudinal and transverse response, we must include realistic nuclear charge and current operators. In figure 3, we show the longitudinal response of the alpha particle at q=400 MeV/c.[19] For present purposes, we transform the measured response to the imaginary-time picture. The experimental points were measured at the Bates and Saclay, respectively. Since the experiments are performed with electrons of finite energy, only a portion of the full response is obtained. The high-energy tails of the response are not available experimentally, and here we have estimated the missing strength as the difference between the short-dashed lines and the points. This missing strength becomes rapidly unimportant to the imaginary time response, it gives essentially no contribution beyond $\tau = 0.015$ MeV^{-1}. The complete MC calculations are shown as a shaded error band in the figure; the calculations are in very good agreement with the measurements. The measured response is dramatically different than that obtained in a simple PWIA picture which ignores final-state interactions.

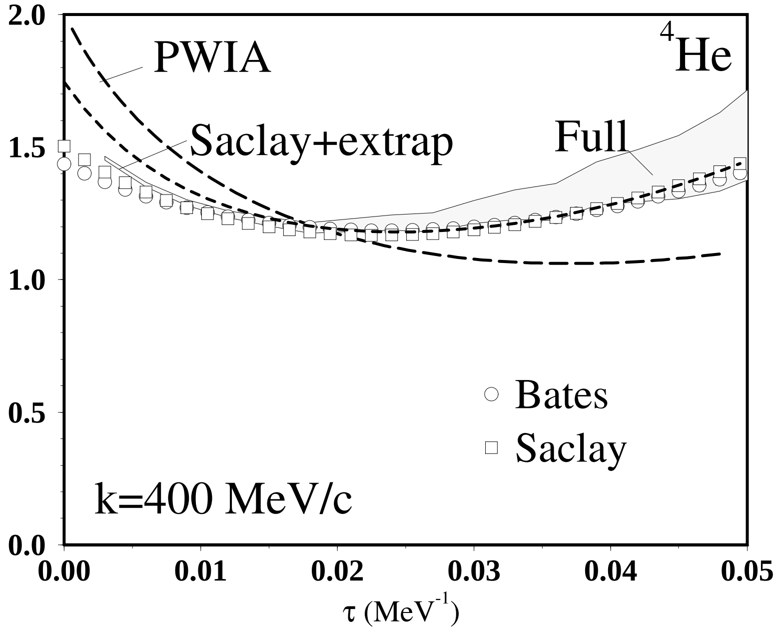

Figure 3. Longitudinal response of the alpha particle; comparison of theory and experiment. The shaded band represents the statistical errors of the calculation. The response is scaled as in the previous figure.

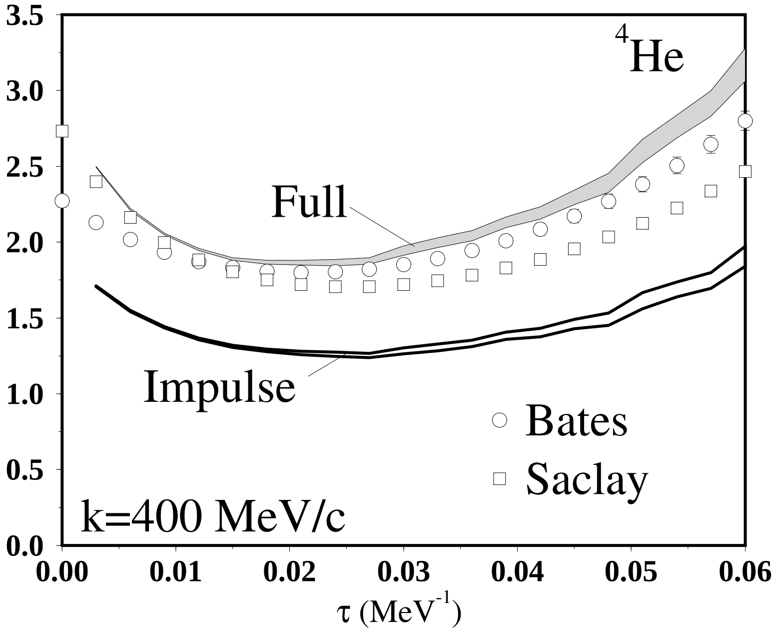

Figure 4. Transverse response of the alpha particle; comparison of theory and experiment.

We display the transverse response in figure 4.[20] Traditionally it had been very difficult to simultaneously obtain the correct magnitudes for both the longitudinal and transverse response. The measured longitudinal/transverse ratio is smaller than would be expected based upon simple PWIA-like models. In the transverse channel, the dominant single-nucleon contribution to the response is from the nucleon's magnetic moment. As the neutrons and protons magnetic moments are of opposite signs, this quantity is largely isovector ($\propto \tau_i^z$) in nature. The longitudinal coupling is dominated by a proton projection operator $(1 + \tau_i^z)/2$, and hence is the sum of an isoscalar and an isovector term. The impulse curve in figure 4 includes only the single-nucleon current. If this were the whole story, the transverse response would be much smaller than the longitudinal response, contrary to experimental results. Indeed, this is the case when considering single-nucleon currents only, as shown in figure 2.

However, current conservation requires a two-nucleon contribution to the transverse response even in lowest non-relativistic order. This contribution is quite important, adding this term to the current gives the difference between the curves labeled 'full' and 'impulse' in the figure. When this two-body current, largely due to pion exchange, is included, the experimental and calculated response curves are in good agreement.

Many other issues in nuclear response remain open, however. For example, it would be very useful to be able to reliably go from the imaginary-time domain to the energy domain. The issues here are precisely the same as in condensed-matter and atomic and molecular physics, and is an area of active research. Experimentally, the response in larger nuclei is still poorly known, due to difficulties in separating the longitudinal and transverse response. Other issues include recent measurements of polarized proton-neutron scattering on Carbon, which have been used to attempt to extract the spin-longitudinal and spin-transverse response. The extracted quantities are not yet understood in terms of a microscopic model. Finally, many recent electron-scattering experiments include measurements of polarization observables; understanding these reactions can be important in trying to extract neutron properties from electron scattering off nuclei. All of these issues are of current experimental and theoretical interest.

9. Summary and Outlook

During the past 10 years, Quantum Monte Carlo methods have been successfully applied to studies of nuclei up to A=8. No other methods are presently available for studying nuclei with A $>$ 4 with realistic nuclear interactions. These studies encompass not only spectra, but also elastic and inelastic form-factors, ground-state correlations, low-energy scattering and capture reactions, and the response of nuclei to a variety of external probes.

In general, there is quite good agreement between theory and experiment. Several unsolved problems remain, however. These include the spectra of neutron-rich nuclei and the $L \cdot S$ splittings in nuclei. One of the important areas for future research is the study of three-nucleon interactions and relativistic effects in light nuclei, with the goal of providing a more accurate picture of the spectra. Once this is accomplished, a comprehensive and completely microscopic study of a variety of intriguing low-energy reactions can be undertaken. Important applications include the solar neutrino reactions and studies parity-violation in the weak interaction through few-nucleon reactions.

Larger systems are also important, of course. Carbon and Oxygen are quite important, for example, both because a variety of important experimental results are available for these nuclei, and because of their complex structure and spectra. There is also a great deal of interest in the properties of neutron and nuclear matter, both at zero and finite temperatures. The response of matter to a variety of external probes is also important both astrophysically and within a nuclear physics context. Microscopic calculations of larger nuclei and matter with realistic interactions remains an outstanding challenge in nuclear many-body theory.

References

1. Carlson, J., and Schiavilla, R., 1998, Structure and Dynamics in Few-Nucleon Systems, *Reviews of Modern Physics* **70**, pp 743-842.
2. Koonin, S.E., Dean D. J., and Langanke, K., 1997, Shell-Model Monte-Carlo Methods, *Physics Letters* **B 367**, pp. 2-77.
3. Machleidt, R., 1989, The Meson Theory of Nuclear-Forces and Nuclear-Structure, *Adv. Nucl. Phys.* **19**, pp. 189-376.
4. B. S. Pudliner, Pandharipande, V. R., Carlson, J., Pieper, Steven C., and Wiringa, R. B., 1997, Quantum Monte Carlo Calculations with A ≤ 7, *Phys. Rev.* **C56**, pp. 1720-1750.
5. Forest, J. L., Pandharipande, V. R., and Friar, J. L.,1995, Relativistic Nuclear Hamiltonians, *Physical Review C* **52**, pp. 568-575.
6. Machleidt, Sammarruca, R. F., and Song, Y., 1996, Nonlocal Nature of the Nuclear-Force and its Impact on Nuclear-Structure, *Physical Review C* **53**, pp. R1483-1487.
7. Lomnitz-Adler, J., Pandharipande, V.R., and Smith, R., 1981, Monte-Carlo Calculations of Triton and ^{4}He Nuclei with the Reid Potential, *Nuclear Physics* **A361**, pp. 399-411.
8. Carlson, J., and Wiringa, R. B., 1991, Variational Monte Carlo Techniques in Nuclear Physics, in *Computational Nuclear Physics Vol 1*, K. Langanke, J. A. Maruhn, and S. E. Koonin, ed., Springer-Verlag, Berlin, pp. 171-189.
9. Cohen, S., and Kurath, D., 1965, Effective interactions for the 1p Shell, *Nucl. Phys.* **73**, pp. 1.
10. Benhar, O., Carlson, J., Pandharipande, V. R., and Schiavilla, R., 1995), Euclidean Responses of ^{4}He at High Momentum Transfer, *Phys. Rev.* **C52**, pp. 2601-2607.
11. Carlson, J., Pandharipande, V. R., and Wiringa, R. B., 1984, Variational Calculations of Resonant States in ^{4}He, *Nucl. Phys.***A424**, pp. 47-59.
12. Carlson, J., Schmidt, K. E., and Kalos, M. H., 1987, Microscopic Calculations of ^{5}He with Realistic Interactions, *Phys. Rev.* **C36**, pp. 27-31.
13. Arriaga, A., Pandharipande, V. R., and Schiavilla R., 1991, Variational Monte-Carlo Calculations of the ^{2}H (d,γ) ^{4}He reaction at Low Energies *Phys. Rev.* **C43**, pp. 983-991.
14. Schiavilla, R., Wiringa, R. B., Pandharipande, V. R., and Carlson, J., 1992, Effects of Delta-Isobar Degrees of Freedom on Low-Energy Electroweak Transitions in Few-Body Nuclei, *Phys. Rev.* **C45**, pp. 2628-2639.
15. Bahcall, John N., and Krastev, Plamen I., 1998, Do *hep* neutrinos affect the solar neutrino energy spectrum?, preprint hep-ph/9807525.
16. Schiavilla, R., Wiringa, R. B., and Carlson, J., 1993, The Coulomb Sum and Proton-Proton Correlations in Few-Body Nuclei, *Phys. Rev. Lett.* **70**, pp. 3856-3859.
17. Jourdan, J., 1996, Quasi-Elastic Response Functions : The Coulomb Sum Revisited, *Nucl. Phys.* **A 603**, pp. 117-160.
18. Forest, J. L., *et al.*, 1996, Femtometer Toroidal Structures in Nuclei, *Phys. Rev.* **C54**, pp. 646-667.
19. Carlson, J., and Schiavilla, R., 1992, Euclidean Proton Response in Light Nuclei, *Phys. Rev. Lett.* **68**, pp. 3682-3685.
20. Carlson, J., and Schiavilla, R., 1994, Inclusive Electron Scattering and Pion Degrees of Freedom in Light Nuclei, *Phys. Rev.* **C49**, pp. R2880-2884.